

Supporting Information

Temperature-Responsive Hydrophobic Silica Nanoparticle Ultrasound Contrast Agents Directed by Phospholipid Phase Behavior

Nicholas T. Blum,¹ Adem Yildirim,^{1,†} Ciara Gyorkos,¹ Dennis Shi,^{1,^} Angela Cai,^{1,‡} Rajarshi

Chattaraj,^{2,+} and Andrew P. Goodwin.^{1}*

¹Department of Chemical and Biological Engineering, University of Colorado Boulder, Boulder, CO 80303 USA

²Department of Mechanical Engineering, University of Colorado Boulder, Boulder, CO 80309 USA

*andrew.goodwin@colorado.edu

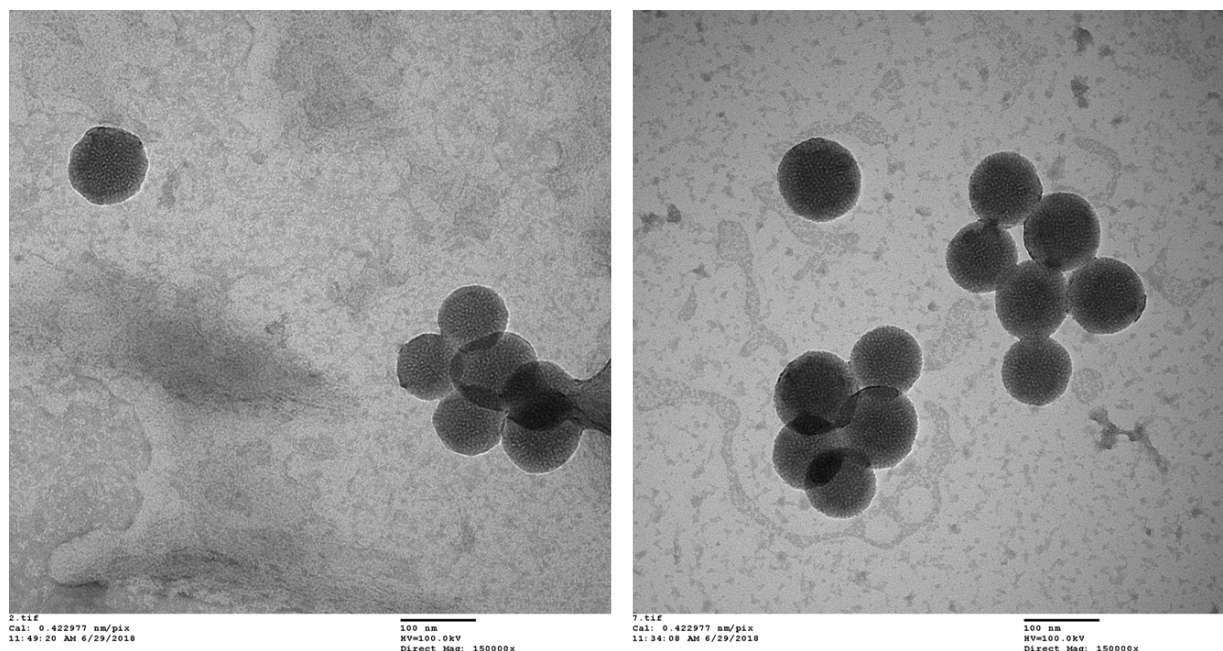


Figure S1. TEM images of (left) DLPC coated hMSNs and (right) DBPC coated hMSNs with 1% uranyl acetate stain.

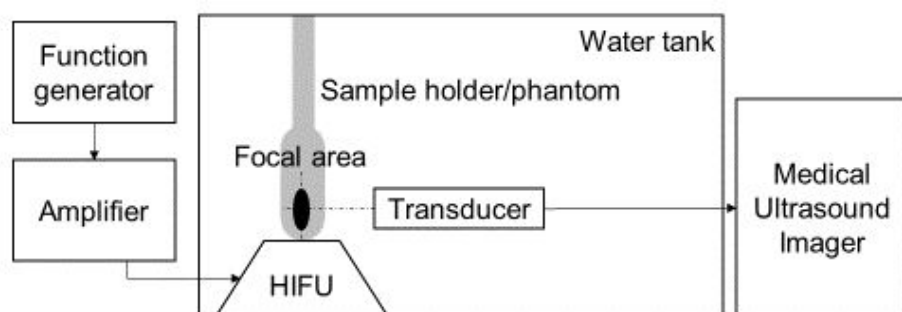


Figure S2. Schematic showing imaging setup. Voltage and HIFU settings are controlled by a function generator, which then feeds through an amplifier and into the HIFU transducer. The transducer emits ultrasound waves that converge in a focal area inside the phantom. Imaging is performed by a transducer aligned orthogonally to the HIFU propagation and is operated by a medical ultrasound machine.

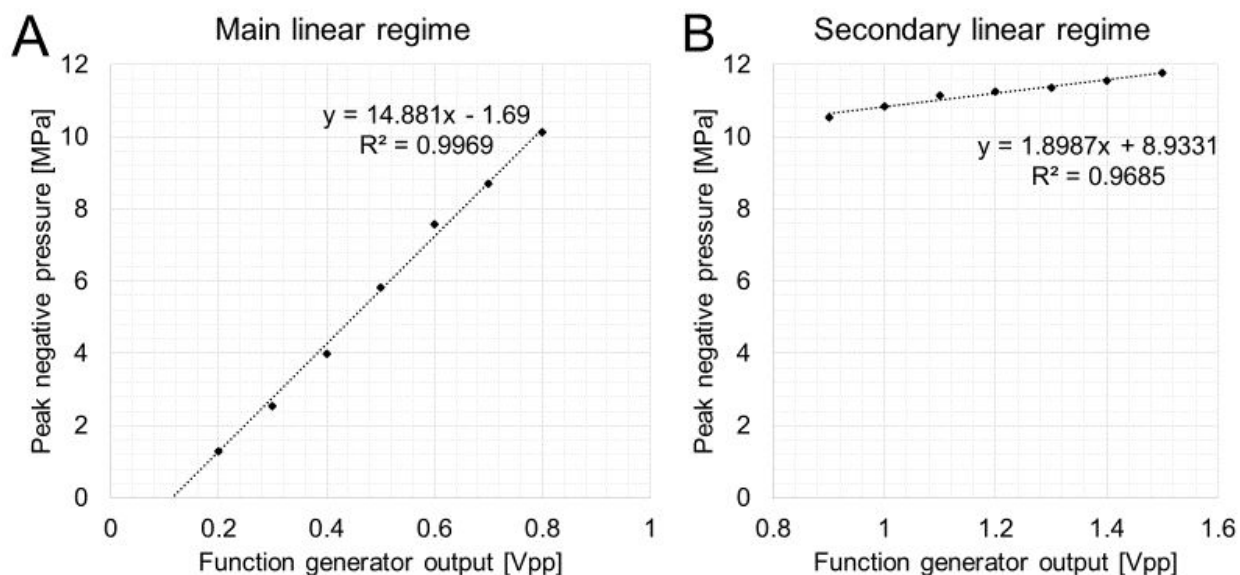


Figure S3. Calibration data showing two linear regimes relating function generator output with measured peak negative pressure in the HIFU focal area. (A) The main linear regime used for function generator voltages from 0.1-0.8 Vpp. (B) Secondary linear regime at higher outputs and used for values between 0.8 and 1.6 Vpp. The decrease in slope is caused by limitations in the total power leaving from the amplifier.

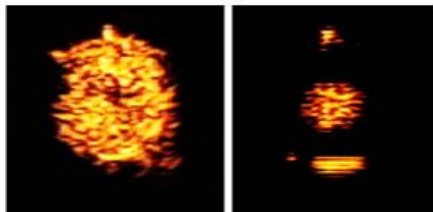


Figure S4. Ultrasonogram images of (left) approx. 10^7 microbubbles per mL in PBS under conditions specified in the main text as compared to (right) 100 $\mu\text{g/mL}$ (approx. 10^{10} particles per mL) of DPPC coated hMSNs.

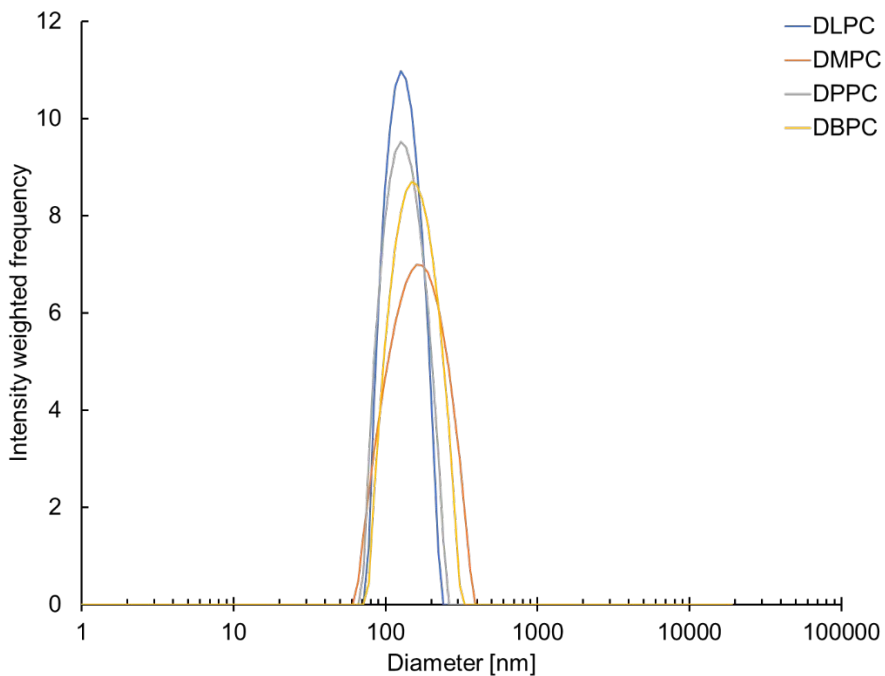


Figure S5. Intensity weighted dynamic light scattering histograms for hMSNs coated with saturated phospholipids of varying tail length: DLPC, C12; DMPC, C14; DPPC, C16; DBPC, C18. Some variability is noted in the size distributions, but no significant changes were observed in overall dispersibility.

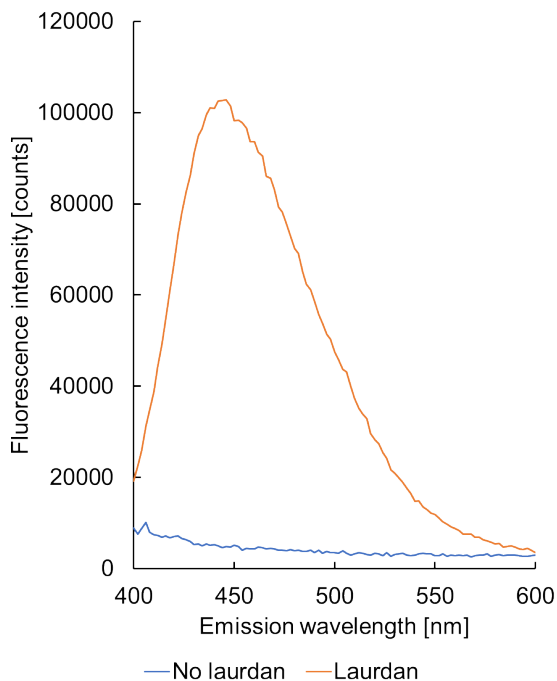


Figure S6. Emission spectra of DPPC-coated hMSNs at a concentration of 0.8 mg/mL with and without the dye laurdan doped at 1 mol% at 370 nm excitation and 20°C.

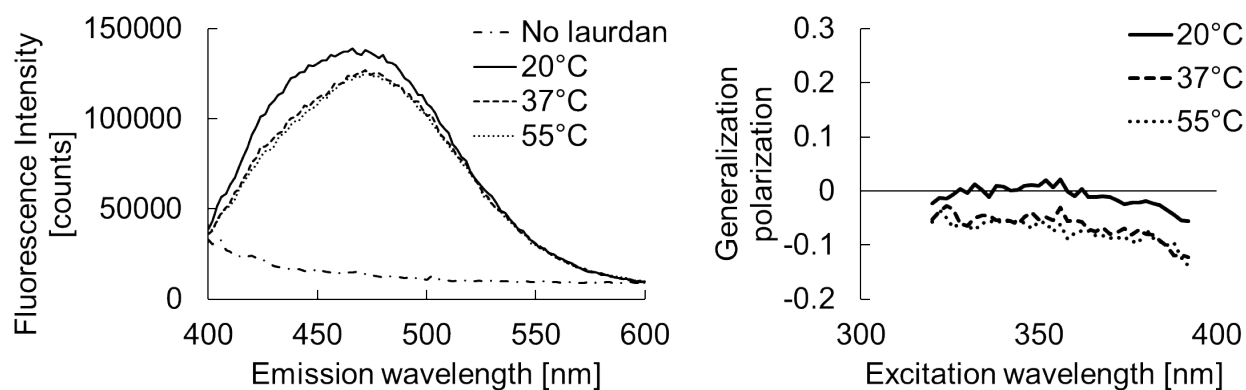


Figure S7. (Left) Emission spectra of DMPC-coated hMSNs with 1 mol% laurdan. The sample without laurdan was acquired at 20°C. (Right) Corresponding GP curves for DMPC-coated hMSNs at the same temperatures. No GP was calculated for the sample without laurdan.

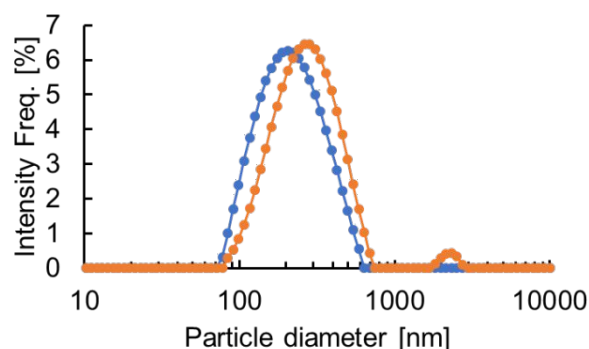


Figure S8. Intensity weighted dynamic light scattering histograms for DPPC coated hMSNs incubated initially in PBS (blue) and washing and then again after washing 3x with PBS (orange). A small amount of aggregation is noted after repeated washing.

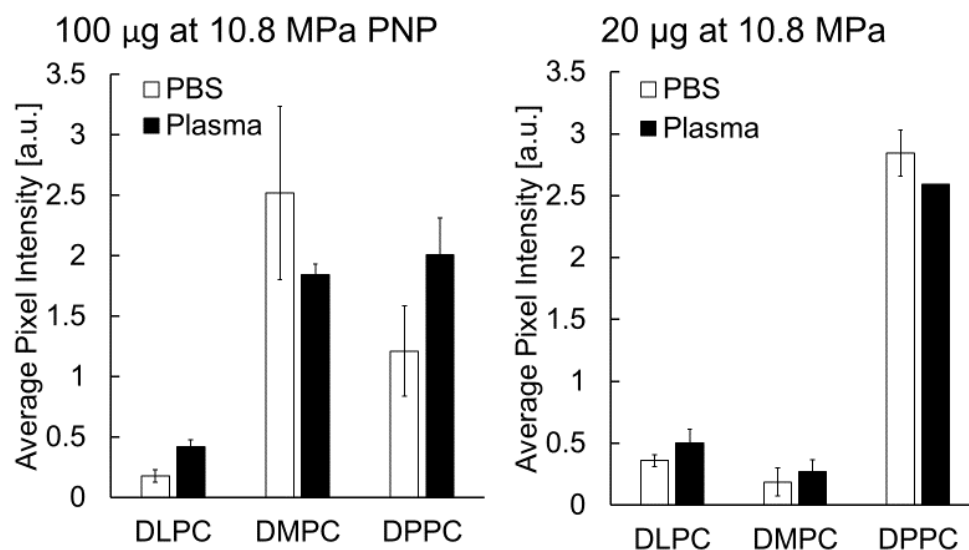


Figure S9. Average pixel intensity for videos of P@hMSNs of different coatings for (left) concentration of 100 µg/mL and (right) 20 µg/mL. The average pixel intensity is an average over the course of a 10 second video of simultaneous HIFU and Sequoia ultrasound imaging, with 1-3 videos taken per condition. Error bars are standard deviation for the average pixel brightness of videos in the region of interest.

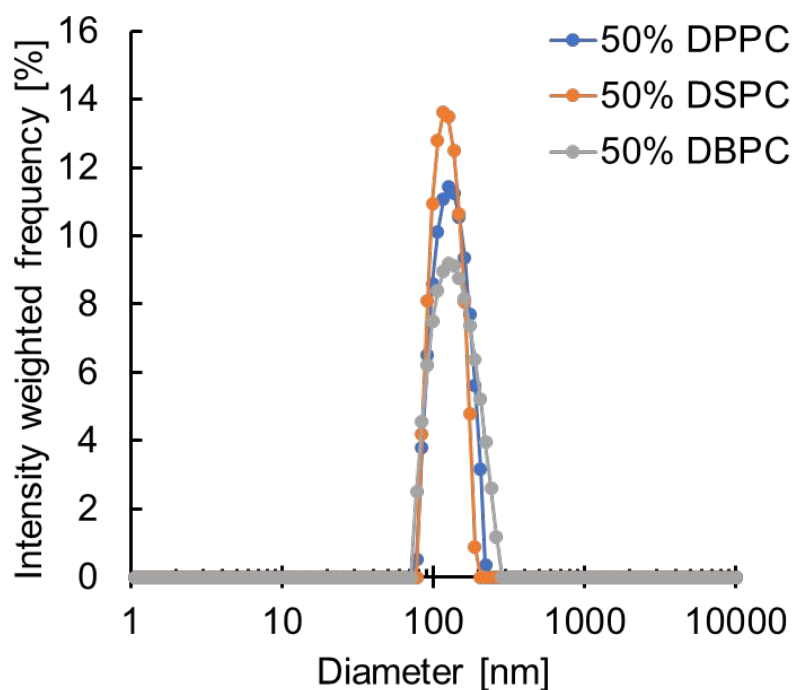


Figure S10. Intensity weighted dynamic light scattering histograms for hMSNs coated with 50% DLPC and the corresponding longer-tailed lipid. No significant changes were found in the dispersibility of the particles with mixed lipid coatings.

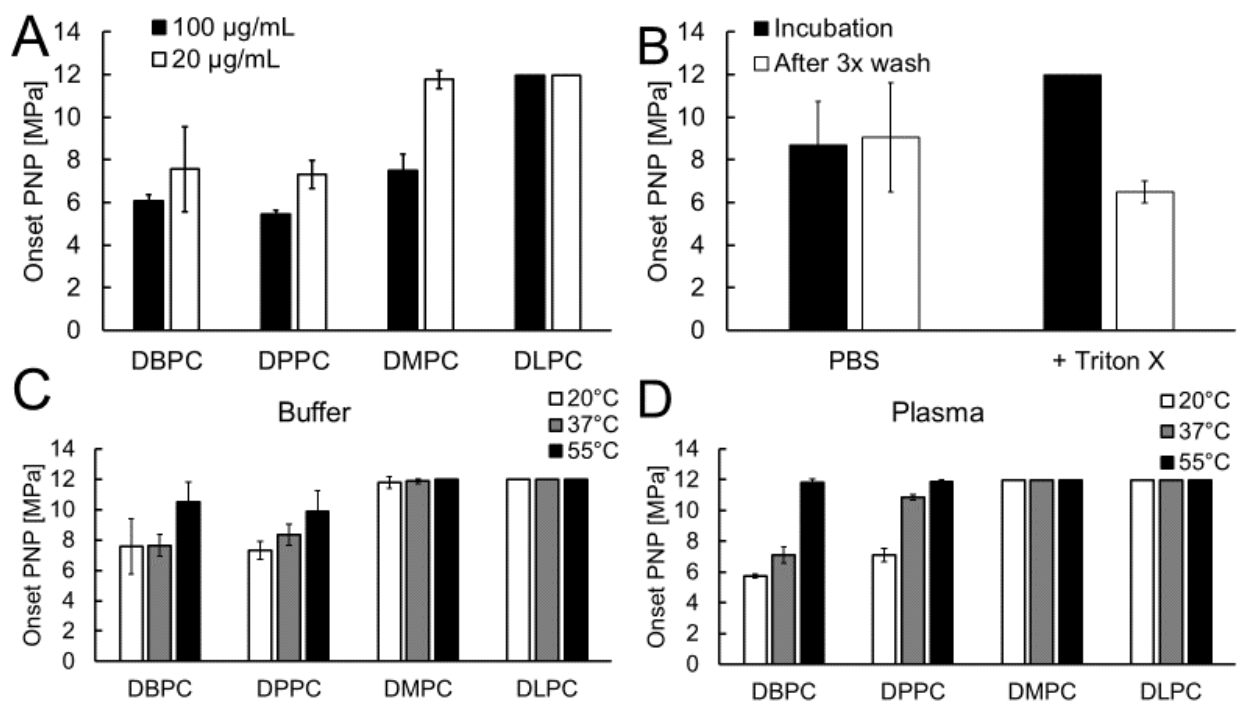


Figure S11. (A) Side-by-side comparison of the acoustic onset for P@hMSNs with different lipids at 100 $\mu\text{g/mL}$ and 20 $\mu\text{g/mL}$. (B) DPPC coated hMSNs at 20 $\mu\text{g/mL}$ with and without Triton treatment as described in the main text. (C) Experiment as described in Figure 1 (right) for a particle concentration of 20 $\mu\text{g/mL}$. (D) Experiment as described for Figure 6 (top) for a concentration of 20 $\mu\text{g/mL}$.